Research in Veterinary Science 106 (2016) 48–55

Contents lists available at ScienceDirect

Research in Veterinary Science

journal homepage: www.elsevier.com/locate/rvsc

Differentiation at necropsy between *in vivo* gas embolism and putrefaction using a gas score

Yara Bernaldo de Quirós [a,*], Pedro Saavedra [b], Andreas Møllerløkken [c], Alf O. Brubakk [c], Arve Jørgensen [c,d], Oscar González-Díaz [e], Jose L. Martín-Barrasa [f,g], Antonio Fernández [a]

[a] Veterinary Histology and Pathology, Department of Morphology, Institute of Animal Health, Veterinary School, University of Las Palmas de Gran Canaria (ULPGC), Trasmontaña s/n, 35416 Arucas, Las Palmas, Spain
[b] Department of Mathematics, University of Las Palmas de Gran Canaria (ULPGC), Campus de Tafira s/n, 35017, Las Palmas, Spain
[c] Department of Circulation and Medical Imaging, Norwegian University of Science and Technology, Trondheim, Norway
[d] Department of Diagnostic Imaging, St. Olavs University Hospital, Trondheim, Norway
[e] Physical and Chemical Instrumental Center for the Development of Applied Research Technology and Scientific estate, Edificio Polivalente 1, University of Las Palmas de Gran Canaria (ULPGC), Campus de Tafira s/n, 35017, Las Palmas, Spain
[f] Multidisciplinary Organ Dysfunction Evaluation Research Network, Research Unit, Hospital Universitario de Gran Canaria, Dr. Negrín, Las Palmas de Gran Canaria, Las Palmas, Spain
[g] Infectious Diseases and Fish Pathology, Institute of Animal Health, Veterinary School, University of Las Palmas de Gran Canaria (ULPGC), Trasmontaña s/n, 35416 Arucas, Las Palmas, Spain

ARTICLE INFO

Article history:
Received 12 July 2015
Received in revised form 19 February 2016
Accepted 7 March 2016
Available online xxxx

Keywords:
Putrefaction
Gas embolism
Decompression
Gas bubbles
Venous gas index
Stranded marine mammals

ABSTRACT

Gas bubble lesions consistent with decompression sickness in marine mammals were described for the first time in beaked whales stranded in temporal and spatial association with military exercises. Putrefaction gas is a post-mortem artifact, which hinders the interpretation of gas found at necropsy. Gas analyses have been proven to help differentiating putrefaction gases from gases formed after hyperbaric exposures. Unfortunately, chemical analysis cannot always be performed. Post-mortem computed tomography is used to study gas collections, but many different logistical obstacles and obvious challenges, like the size of the animal or the transport of the animal from the stranding location to the scanner, limit its use in stranded marine mammals. In this study, we tested the diagnostic value of an index-based method for characterizing the amount and topography of gas found grossly during necropsies. For this purpose, putrefaction gases, intravenously infused atmospheric air, and gases produced by decompression were evaluated at necropsy with increased post-mortem time in New Zealand White Rabbits using a gas score index. Statistical differences ($P < 0.001$) were found between the three experimental models immediately after death. Differences in gas score between *in vivo* gas embolism and putrefaction gases were found significant ($P < 0.05$) throughout the 67 h post-mortem. The gas score-index is a new and simple method that can be used by all stranding networks, which has been shown through this study to be a valid diagnostic tool to distinguish between fatal decompression, iatrogenic air embolism and putrefaction gases at autopsies.

1. Introduction

Gas bubble lesions consistent with decompression sickness in marine mammals were described for the first time in beaked whales that mass stranded in temporal and spatial association with military exercises where mid-frequency sonar was used (Jepson et al., 2003; Fernandez et al., 2005). Since this report, there has been an increasing body of evidence showing the presence of gas bubbles in both live and dead marine mammals (Moore and Early, 2004; Moore et al., 2009; Dennison et al., 2012; Bernaldo de Quirós et al., 2011, 2012a; Jepson et al., 2005).

The presence of intra- and extra-vascular gas bubbles can give important information about the cause of death in forensic investigations. Its presence on the venous side of the circulatory system is called venous gas embolism (VGE). VGE can occur due to different causes such as accidents related to surgical procedures (Muth and Shank, 2000), penetrating trauma, air injection as a criminal intervention, barotraumas (Knight, 1996), or gas-phase separation in the body from supersaturated tissues after a reduction of ambient pressure (decompression) in divers, tunnels workers, aviators, astronauts (Hamilton and Thalmann, 2003), marine mammals (Fernandez et al., 2005), and sea turtles (García-Párraga et al., 2014). When gas

* Corresponding author at: Institute of Animal Health, Instituto Universitario de Sanidad Animal, Veterinary School, University of Las Palmas, Facultad de Veterinaria, C/ Trasmontaña s/n, 35416 Arucas, Las Palmas, Spain.
E-mail addresses: ybernaldo@becarios.ulpgc.es (Y. Bernaldo de Quirós), saavedra@dma.ulpgc.es (P. Saavedra), andreas.mollerlokken@ntnu.no (A. Møllerløkken), alfb@ntnu.no (A.O. Brubakk), arve.jorgensen@ntnu.no, arve.jorgensen@stolav.no (A. Jørgensen), oscar.gonzalez@ulpgc.es (O. González-Díaz), joseluis.martin@ulpgc.es (J.L. Martín-Barrasa), afernandez@dmor.ulpgc.es (A. Fernández).

http://dx.doi.org/10.1016/j.rvsc.2016.03.007
0034-5288/

embolism is suspected as a cause of death, it is important to determine the origin and cause of gas embolism. The main problem in these cases is to differentiate between gas embolism and gases produced *post-mortem* (PM) due to putrefaction, especially when working with stranded marine mammals since the time of death is frequently unknown.

Specific procedures for cases in which gas embolism is suspected are followed at autopsies: Computed Tomography (CT) or other imaging techniques are performed as a pre-autopsy step for observation and localization of gas bubbles (Knight, 1996; Varlet et al., 2015), dissection is done according to Richter technique (Richter, 1905), and gas is collected from the heart for analytical purposes (Varlet et al., 2015; Bajanowski et al., 1998). Gas composition analyses are used to differentiate between gas embolism and putrefaction gases (Bajanowski et al., 1998; Varlet et al., 2014; Bernaldo de Quirós et al., 2013a). These analyses are effective before a threshold PM time, making it critical to perform autopsies in a timely manner (Bernaldo de Quirós et al., 2013a).

Gas composition analyses have been successfully performed in marine mammals to distinguish between putrefaction gases and gas embolism (Bernaldo de Quirós et al., 2012a; Bernaldo de Quirós, 2011; Bernaldo de Quirós et al., 2013b). However, this method requires trained personnel, and is time sensitive, and limited if samples have to be shipped across long distances (Bernaldo de Quirós et al., 2011, 2012b).

Marine mammals may strand on inaccessible coasts where transport of the carcass is not an option, thus the necropsy must be performed *in situ*. There are very few CT scanners available for use on wild marine mammals. Their location (usually far from the stranding place) and the size of the animal, for instance medium to large cetaceans, such as beaked whales, will not fit in most scanners, limit the use of this technique in stranded marine mammals. Currently, a standardized method to characterize the amount and distribution of gas bubbles in veins and tissues observed grossly during necropsies of marine mammals has been proposed but has not been validated (Bernaldo de Quirós et al., submitted for publication). This method would allow for the comparison of gas amount among individuals, and differentially diagnose "*in vivo*" gas embolism from putrefaction gases.

In this study we test this index-based methodology for characterizing the presence and volume of gas bubbles present in a body, providing a new low cost and accessible diagnostic method to all marine mammal stranding networks worldwide. In order to test and validate the methodology, individual, environmental variables and PM time must be controlled, thus an animal model with New Zealand White Rabbits (NZWR) was used. For this purpose, gas presence, amount, and distribution macroscopically visualized were grossly characterized during necropsies of NZWR using a relative index with three experimental models: putrefaction gases, experimental infused air embolism (AE), and a hyperbaric compression/decompression (C/D) model. The results obtained with the gas score index were compared with the analytical results of the gas composition of the bubbles for validation (Bernaldo de Quirós et al., 2013a).

2. Material and methods

A total of 41 NZWR (3179 ± 419 g) were used for the experiments. The animals were provided by the Animal Supply Center of Dr. Negrín Hospital, Spain, and the Norwegian University of Science and Technology, Norway. All experiments were performed in accordance with the European Union regulations for laboratory animals. Experimental protocols were approved by the Ethical Committee for Animal Experiments of Dr. Negrín hospital (ref. CEEBA 005/2010) and by the Norwegian Committee for Animal Experiments. Experiments were performed under surgical anesthesia (Medetomidine of 0.5 $mg \cdot kg^{-1}$, and Ketamine of 25 $mg \cdot kg^{-1}$, subcutaneously).

The animals were divided into three experimental groups: (1) control or experimental putrefaction model (n = 10), (2) infused AE model (n = 11), and (3) C/D model (n = 20). Each animal received a different treatment based on its group (see experimental procedures). As a result of the treatment the animals died. Animals were stored in hermetically sealed plastic boxes for biological material at room temperature during different times. Necropsies were performed on these animals to look for gas presence (See PM procedures). Gas amount was evaluated using an index proposed by Bernaldo de Quirós et al. (2013c). Additionally gas composition analyses were performed to contrast and validate the results obtained with the index method (Bernaldo de Quirós et al., 2011).

2.1. Experimental procedures

2.1.1. Infused AE model

AE was induced by venous atmospheric air infusion through a catheter (0.36 mm I.D.) placed in the marginal ear vein. A pump was used to administer the air at 2.2 $mL \cdot min^{-1}$ until expiration. Rabbits died within 2 to 6 min, as a result, the total volume of infused air varied between 4.5 and 13.0 mL. Dead animals were stored at room temperature (24.8 ± 0.6 °C) for 0, 20 and 40 min, and 1, 3, 6, 12, 27, 42, 53, and 67 h PM (n = 1 for each time).

2.1.2. Compression/decompression model

Anesthetized NZWR were compressed in pairs in a dry, hyperbaric chamber (Animal Chamber System, NUT, Haugesund, Norway) to 810.6 kPa, during a bottom time of 45 min, and followed by a rapid linear decompression (0.33 $m \cdot s^{-1}$) to one atmosphere. The diving protocol was selected to induce severe decompression stress with excessive amounts of intra-corporal gas formation. Eleven out of twenty animals died within 1 h after decompression. Animals that survived for 1 h after decompression were euthanized with an intraperitoneal injection of 200 $mg \cdot kg^{-1}$ diluted pentobarbital. The bodies were stored at room temperature (23.1 ± 1.3 °C) for 0, 20 and 40 min, and 1, 3, 6, 12, 27, 42, and 67 h PM (n = 2 for each time). Only those animals that died due to hyperbaric decompression were included in the model (n = 11).

2.1.3. Experimental putrefaction model

Ten NZWR were euthanized with an intraperitoneal injection of 200 $mg \cdot kg^{-1}$ diluted pentobarbital. Euthanized animals were stored at room temperature (23.4 ± 0.8 °C) for 1, 3, 6, 12, 27, 42, 47, 53 (n = 1 for each time), and 67 (n = 2) hours PM prior to necropsy. The PM time prior to necropsy was initially planned to be identical in the putrefaction model to the infused AE and Compression/Decompression models. However, putrefaction gas bubbles were absent at 6, 3 and 1 h PM. Thus, no experiments were carried out at 0, 20, and 40 min PM in order to reduce the number of rabbits used following ethical standards.

2.2. PM procedures

Complete necropsies were carried out for each animal at its scheduled PM time. In addition to PM time a decomposition code from 1 to 5, based on the conservation state of the body and internal organs, was given to each animal (Kuiken and García-Hartmann, 1991). Decomposition codes allow for the comparison between different individuals that were examined at different PM times, exposed to different environmental conditions during that time, but that shared the same decomposition status (Kuiken and García-Hartmann, 1991; Geraci and Lounsbury, 2005). Thus, decomposition codes were used in addition to PM time in this study, although efforts were made to preserve the bodies at similar environmental conditions.

Necropsy was performed with the rabbit in dorsal *decubitus* position. Dissection was carefully done to avoid severing any large vessels. Initially, the skin was removed and the subcutaneous veins were examined for the presence of gas bubbles. Then the abdominal cavity was opened, and the mesenteric veins as well as the vena cava were examined.

Finally, the thoracic cavity was opened, allowing access to the heart. Throughout the necropsy, photos were taken of detected intra- and extra-vascular gas bubbles.

The presence of intra and extra-vascular gas bubbles was characterized using a gas score index following Bernaldo de Quirós et al. (2013c). This index-based method consists of giving a gas score from 0–VI to different vascular locations: subcutaneous veins, femoral veins, mesenteric veins, inferior vena cava, coronary veins and to the right atrium (Table 1). In addition a gas score from 0–III is used to describe the presence of extravascular gas, beneath the capsule of different organs (subcapsular emphysema), and in adipose tissues (interstitial emphysema) (Table 2). The total gas score is finally calculated by the summation of the gas scores for each defined vascular location in addition to the subcapsular and interstitial emphysema gas score. Total gas score in each animal ranges from 0 to 42 (Table 3).

After gas scoring, the animals were completely submerged in water for collection and later analysis of the gas composition (Bernaldo de Quirós et al., 2013a).

2.3. Statistical analysis

Data were analyzed using the "R" data analysis software, version 2.11.1.

A model for the evolution of the summation of gas scores against PM time and treatment was proposed. Exploration of the data showed a linear pattern of variation for putrefaction and a logarithmic growth pattern for the other two treatments. Thus, the proposed model has the form:

$$GS = \mathrm{a} + \tau_A A + \tau_D D + \beta_P P \cdot hours + \beta_A A \cdot \log(1 + hours) + \beta_D D \cdot \log(1 + hours) + \varepsilon \quad (1)$$

where GS represents the gas score, P, A and D are 0–1 variables indicating the used treatment (putrefaction, induced AE and C/D respectively) *hours* represents the PM time and finally ε is the error term, which has a mean of zero and a variance constant. Parameters τ_A and τ_D correspond to the expected increase of the gas score for the induced AE and C/D models respectively in relation to putrefaction treatment at zero hours. The model was fitted by the least squares method. The estimation of the parameters was expressed by 95% confidence intervals. The goodness of fit was assessed using the corrected coefficient R^2. Statistical significance was set at $P < 0.05$.

Table 1
Gas score index for intravenous bubbles.

Gas score	Definition
0	**Absence of gas bubbles** within venous vessels (Fig. 1a, d, g).
I	**Occasional small bubble** found by carefully screening of venous vessels (Fig. 1b).
II	**Few bubbles:** Gas bubbles are more easily found but a careful screening of different venous vessels and sections of the veins is also required. The quantity of gas bubbles is easy to count. In addition, small "discontinuities of blood" can be present. These discontinuities of blood are small sections of veins showing absence of red cells and associated haemoglobin but with clear liquid instead, presumably plasma from which the red cells have retracted. There is no evidence of gas in these sections, and the veins show different grades of collapse.
III	**Few bubbles but larger discontinuities of blood**.
IV	**Moderate presence of gas bubbles** within a specific vein (Fig. 1h). The presence of gas bubbles is obvious at this score, and a careful screening for localized gas bubbles is no longer necessary. Counting gas bubbles would be a tedious but possible task.
V	**Abundant presence of gas bubbles** (Fig. 1i); many gas bubbles of different volumes would be present within the same vein making quantification of bubbles very difficult, if not impossible.
VI	**Complete sections of vessels filled with gas** (Fig. 1c, e, f). This occurs by the coalescence of gas bubbles. Quantification of bubbles is no longer possible.

Table 2
Gas score index for extravascular gas underneath the organs' capsules and in adipose tissues.

Gas score	Definition
0	**Absence of gas.**
I	**Scarce presence of gas:** only in one organ or anatomic region.
II	**Moderate presence of gas:** affecting two or three organs or anatomic regions.
III	**Abundant presence of gas:** affecting many different organs. Systemic.

Using the calculated model, we tested whether the expected values of the gas score from the AE model (Eq. (2)) and from the C/D model (Eq. (3)) were significantly higher along the observation time with a confidence interval of 95% using the following equations for the expected values:

$$E\,[GS\,|hours = h, treat = AE]\text{-}E[GS|\ hours = h, treat = P] = \tau_A + \beta_A \log(1 + h) - \beta_P h \quad (2)$$

$$E\,[GS\,|hours = h, treat = C/D]\text{-}E[GS|\ hours = h, treat = P] = \tau_D + \beta_D \log(1 + h) - \beta_P h \,\mathrm{In}. \quad (3)$$

In addition, the correlation between PM time (hours) and decomposition codes was studied using Pearson coefficient (r).

3. Results

The flux of gas bubbles was documented using a gas score index in 41 NZWR throughout a period of 67 PM hours.

3.1. Gross findings

3.1.1. Experimental putrefaction model

In the putrefaction model bubbles were absent in most animals or present in small numbers in others that were examined within 12 h PM (Fig. 1a, d, g). These animals were very fresh, not showing coloration changes in any tissue; hence they were assigned with decomposition code 2. The first bubbles were observed at 6 h PM in the mesenteric veins. Only two bubbles were found at this time. At 12 h PM, several small blood discontinuities could be observed in the mesenteric veins, but still only one or two gas bubbles were observed. In the subcutaneous veins a single bubble was found. The intestine showed small gas-inflated sections.

The animals examined after 27 PM hours presented with a few more bubbles. A decomposition code 3 was given to the animals examined at this PM time based on changes in the coloration of the abdominal viscera and because of the moderately friable state of some organs such as the intestine, stomach, liver, and spleen, although the organ's structures were still intact. The caecum was gas-distended. The adipose tissue surrounding the kidney and the coronary fat presented with an emphysematous appearance. Small discontinuities in the blood were observed in the subcutaneous and mesenteric veins. A few bubbles were found in the femoral vein and in the vena cava. Gas bubbles were not observed in the coronary veins or right atrium. Aspiration of the right cardiac ventricle showed absence of gas.

At 42 h PM, decomposition code 4, gas (0.5 mL) was recovered from the right cardiac ventricle for the first time. Decomposition code 4 was designated to this PM time based on changes of coloration in most tissues, including subcutaneous and thoracic cavity tissues. The brain and all abdominal organs were moderately-severely friable. The digestive tract had lost its structure in some areas causing the presence of food in the abdominal cavity. Both the heart and lungs presented with a homogenous reddish-brown color and were slightly friable. Large blood discontinuities and a few bubbles were observed in most veins, including the subcutaneous, femoral, mesenteric veins, and the vena

Table 3
Illustration of the establishment of the gas score for each animal. Abbreviations: v, veins.

Identification	Subcutaneous v.	Mesenteric v.	Femoral v.	Vena cava	Right atrium	Coronary v.	Interstitial emphysema in fatty tissue	Subcapsular emphysema	Total
Animal n	0–VI	0–VI	0–VI	0–VI	0–VI	0–VI	0–3	0–3	0–42

cava. Of importance is the fact that there continued to be an absence of gas bubbles in the coronary veins up to 42 h PM. An accumulation of gas could be observed underneath the capsule of the liver (subcapsular emphysema).

Finally, at 67 h PM (decomposition code 5), a moderate to abundant amount of gas bubbles was observed in the cardiovascular system, except for the coronary veins. Using an aspirometer, up to 0.9 mL and 0.6 mL of gas were recovered from the right and left cardiac ventricles respectively. Subcapsular gas was observed in several organs. The largest subcapsular gas volumes were found in the liver and kidneys. Interstitial emphysema was observed in all adipose tissues of the animal.

3.1.2. Experimental infused AE model

In the AE model gas bubbles were first observed in the right atrium and in the coronary veins. Gas bubbles could be observed in the right atrium because it is slightly translucent and was gas-distended. Immediately after death and 20 min later, bubbles were not observed in other tissues. The gas sampled from the right and left cardiac ventricles (0.6–0.8 mL) was recovered as foam. At 40 min PM, abundant gas bubbles were observed in the vena cava and up to 8 mL were recovered from the right cardiac ventricle. One mL of gas was recovered from the left cardiac ventricle. Gas was recovered as a clean gaseous phase well separated from the liquid phase. After one hour, gas bubbles were widely disseminated in the circulatory vascular system in large volumes,

Fig. 1. Photos from fresh animals (with a maximum of 12 h PM) illustrating the flux of gas bubbles in different locations of the circulatory system (shown in columns) for each experimental model (shown in rows). Appearance of the subcutaneous veins of animals from the putrefaction (a), infused AE (b) and C/D model (c). Appearance of the Vena Cava in the putrefaction (d), infused AE (e) and C/D model (f). Appearance of the mesenteric veins in the putrefaction (g), infused AE (h) and C/D model (i). Gas scores given to each illustration are: gas score 0 (a, d and g), gas score 1 (b), gas score 4 (h), gas score 5 (i) and gas score 6 (c, e, and f). Arrows in (c) are indicating a subcutaneous vein full of gas. Arrows in (d, e, and f) are indicating the location of the vena cava.

except for the subcutaneous veins where an absence or scarce presence of bubbles was observed (Fig. 1b, e and h). At 12 h PM gas bubbles were observed in large quantities in the subcutaneous veins. At this time the adipose tissue started to acquire an emphysematous appearance. Subcapsular gas was not observed until 27 h PM. The average volume of gas recovered from all animals exposed to induced air embolism was 2.6 ± 2.5 mL from the right cardiac ventricle and 0.4 ± 0.4 mL from the left cardiac ventricle. Two out of eleven spleens were slightly larger compared to the others and presented small and numerous bubbles that could be externally observed, resembling a sponge.

3.1.3. Compression/decompression model

Examinations of the animals immediately after their death because of decompression showed gas bubbles widely dispersed and in large volumes in the entire circulatory system, including peripheral veins (Fig. 1c, f, i). Emphysema in the adipose tissue (abdominal adipose tissue and coronary fat) was copious. These findings were the same for all animals regardless of observation time. In several animals the heart was found gas-distended. Those sections of veins that were not filled with gas were very congestive. Multiple haemorrhages could be grossly observed in different tissues and organs such as subcutaneous tissue, abdominal adipose tissue, mesentery, spleen, kidneys, lungs, or heart. The largest volume recovered from the right cardiac ventricle was 12 mL. The average gas volume recovered from the right cardiac ventricle was 5.2 ± 3.4 mL and 0.6 ± 0.5 mL from the left cardiac ventricle. Three out of eleven spleens were completely distended by gas, resembling air balloons.

PM results of the animals that survived for one hour after decompression and were subsequently euthanized were similar to the putrefaction model.

3.2. Gas score

The calculated model for the evolution of summation of gas scores against PM time and treatment had a good fit (adjusted $R^2 = 0.90$) (Fig. 2) (Table 4). It showed statistical difference ($P < 0.001$) of gas score between the three models at time zero (Table 4). Calculated initial levels of gas score for the infused AE model were 12.0 units (95% CI = 6.3; 17.7) higher than the putrefaction model, and those from the C/D model were 33.1 units (95% CI = 27.7; 38.5) higher than the putrefaction model, and 21.1 units (95% CI = 15.8; 26.4) higher than the infused AE model (Fig. 3). Both AE and C/D models were statistically different ($P < 0.05$) from the putrefaction model throughout the 67 PM hours (Fig. 3). However, this difference decreased with PM time.

Putrefaction gases were calculated to grow linearly ($P < 0.001$), at a rate of 0.4 units per hour (95% CI = 0.3; 0.5), while the gas in the infused AE model grew logarithmically ($P < 0.001$; 95% CI = 4.7; 7.8). In contrast, there was a non-significant ($P = 0.205$) logarithmic growth of gases from decompression because the start and the end values were similar (Fig. 2).

Correlation results between PM time and decomposition code showed that these variables have a strong positive linear correlation ($r = 0.959$; $P < 0.001$), meaning that these variables could be used independently and that they have the same predictive value.

Table 4
Estimated model for gas index growth over time adjusted $R^2 = 0.8982$.

Parameter	Estimation (SE)	*P*-value
α	−0.797 (2.090)	0.7061 (NS)
τ_2 (difference between AE and P at time 0)	11.986 (2.913)	<0.001
τ_3 (difference between C/D and P at time 0)	33.112 (2.739)	<0.001
β_1(growing rate for P)	0.409 (0.051)	<0.001
β_2 (growing rate for AE)	6.228 (0.793)	<0.001
β_3 (growing rate for C/D)	1.051 (0.808)	0.2047 (NS)

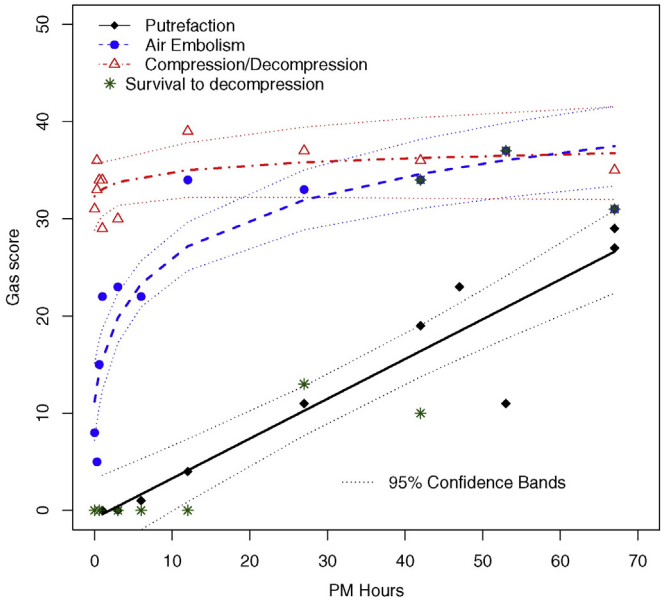

Fig. 2. Plot of the total gas score of each animal (raw data) and the predicted model with 95% confidence interval against the PM time at which the animal was examined. The data of the putrefaction model are presented with black rhombuses. The infused AE model data are presented with blue circles, the C/D model data are presented with red triangles, and the animals from the C/D model that survived for 1 h after decompression and were euthanized, thus excluded from the model, are represented with green asterisks. (For interpretation of the references to color in this figure legend, the reader is referred to the web version of this article.)

4. Discussion

The gas score method allows for differentiation between putrefaction gases, air embolism, and gases formed in response to decompression from hyperbaric exposures. Significant differences for gas score between the three models at time zero were found (Fig. 2). The amount of gas produced because of a fatal decompression was consistently close to the maximum gas score. This gas was widely distributed, including peripheral veins and adipose tissue (Fig. 1). This was the main difference when comparing the C/D model to the AE model. Differences among the three models decreased with PM time as putrefaction gases were produced (Figs. 2 and 3). The putrefaction model did not show a relevant gas score compared to the AE or C/D model until after 27 PM hours (Fig. 2), in agreement with gas composition analyses performed on the same animals (Bernaldo de Quirós et al., 2013a).

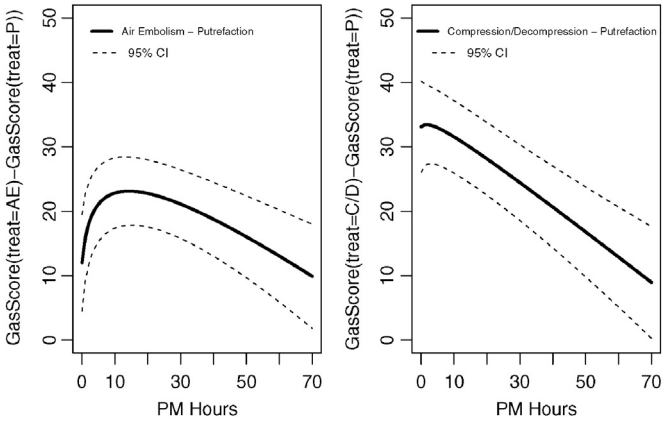

Fig. 3. Expected difference in the gas score between the AE (a) and C/D model (b) compared to the putrefaction model along PM time with a CI of 95%.

4.1. Putrefaction model

Decomposition codes had a strong correlation with PM time, meaning that decomposition code and PM time had the same predictive value. The advantage of decomposition coding is that it allows for the comparison between different individuals that are within the same decomposition code, regardless of the PM time and environmental conditions.

The complete absence of gas bubbles in rabbits necropsied immediately or within a few PM hours (decomposition code 2) is the most important result obtained from the putrefaction model. It indicates that a certain level of putrefaction must be reached in order to produce enough gas to favor gas phase separation from fluids, or at least to be large enough to be macroscopically detected. These negative results also indicate that proper dissection techniques do not introduce air bubbles.

In the putrefaction model gas scores were very low during the first PM hours. Moderate scores were reached after 27 h PM. Gas composition analyses performed on the same animals (Bernaldo de Quirós et al., 2013a) showed statistical differences in composition of the gas up to 27 h PM. After this time putrefaction gases would mask the original gas composition of the emboli. Putrefaction gases were characterized by the presence of hydrogen. Hydrogen was found in most of the samples taken after 27 h PM, but it was absent in fresher samples (Bernaldo de Quirós et al., 2013a). Therefore, both the gas score method and gas analysis are showing similar results and they indicate the importance of performing autopsies in a timely manner in cases where air embolism or diving accidents are suspected.

4.2. AE and C/D model

In the air embolism model, gas score increased during the first PM hours, suggesting that the dissolved gas carrying capacity of the blood might be higher during circulation than in a static mode. Thus, some of the gas would come out from solution once the blood circulation has stopped (PM off-gassing). An alternative or complementary explanation would be that microscopic bubbles might coalesce to form larger macroscopic gas bubbles. This could not be observed as clearly in the C/D as in the AE model; the animals that died because of decompression showed gas score values close to the maximum scale of the scoring method.

Gas in the spleen was observed in two out of eleven animals in the AE model and in three out of eleven in the C/D model, but never in the putrefaction model (zero out of ten). The presence of gas in the spleen, both in the AE and in the C/D model, suggests that it is more likely due to an *in vivo* gas accumulation rather than *in situ* bubble formation.

4.3. Particularities of the C/D model

The C/D model presented some particularities, differing from the AE and putrefaction models. This is the only model in which gas bubbles were observed in the peripheral veins as well as in the adipose tissue immediately after death (Fig. 1). Similar findings have been previously described in other species such as mice, rats, pigs, and rabbits (including NZWR), that have been rapidly decompressed following exposure to high pressures (Eggleton et al., 1945; Lever et al., 1966; Shim et al., 1967). This quality of the C/D model might be due to how bubbles are formed in response to decompression. Bubbles are hypothesized to grow from pre-existing gas nuclei that might be attached to the endothelial layer in the vascular periphery (Harvey, 1945). Bubbles from the vascular periphery would eventually dislodge from the vessel walls and wash out into the central venous vessels, where bubbles would coalesce and increase in size. In addition, the observation of emphysema in the abdominal adipose tissue of these animals suggests the formation of bubbles within tissues reaching first peripheral veins and later central veins. Furthermore, bubbles in the adipose tissue of mice have been reported to grow steadily *in situ* after decompression (Lever et al., 1966). In contrast, in iatrogenic AE cases, gas would enter into the vascular system only through a specific location.

4.4. PM offgassing and implications of the method

The interpretation of PM gas bubble findings has been widely discussed (Varlet et al., 2015; Brown et al., 1978; Cole et al., 2006; Laurent et al., 2011; Laurent et al., 2014; Yokota et al., 2009; Wheen and Williams, 2009). Some authors considered these findings to be artifacts from putrefaction, attempted resuscitation, or PM offgassing (Brown et al., 1978; Cole et al., 2006; Laurent et al., 2011; Wheen and Williams, 2009). In all these cases the presence and topography of the gas in the body were studied using different imaging techniques, but very few attempts were made to estimate the volume of the gas (Varlet et al., 2015; Brown et al., 1978; Laurent et al., 2014). The study of presence or absence of PM gas has been demonstrated to be of poor predictive value to diagnose diving fatalities in experimental models and humans (Varlet et al., 2015; Brown et al., 1978; Cole et al., 2006; Laurent et al., 2011, 2014; Wheen and Williams, 2009). In contrast, gas amount was more useful for this goal (Cole et al., 2006; Laurent et al., 2014).

When using animal models to test diagnostic forensic tools it is crucial that the animals died because of the cause of death being studied. Additionally, in order to simulate a human dive and its corresponding degree of tissue's saturation in an animal model, previous empirical studies or mathematical modeling should be carried out to find the dive that will cause similar results in the selected animal model. All the previous papers using animal models (Brown et al., 1978; Cole et al., 2006; Laurent et al., 2011) failed to fulfill one or both requirements. In the current study, a diving profile causing fatal decompression was chosen in order to validate a forensic methodology to diagnose decompression as the cause of death. Only the animals that died after hyperbaric decompression were included in the model.

To the author's knowledge, this is the first study that has estimated qualitatively the PM presence of gas found grossly during necropsies in different vascular and extravascular locations, and has contrasted its results with gas composition analyses (Bernaldo de Quirós et al., 2013a). The performance of necropsies at different PM times enabled the study of putrefaction gases and PM offgassing.

PM offgassing was only detected during the first PM hours in the AE model. Since in this model atmospheric air was infused intravenously, tissues were not saturated. A possible explanation for this observation is that blood in circulation must be able to hold more dissolved gas than in static mode: blood pressure created by a pumping heart decreases after death, altering surface tension, thus microscopic gas bubbles could grow and coalesce.

The gas scoring (*i.e.*, gas amount) was found to be statistically significant higher in both the AE and C/D model compared with the putrefaction model throughout the 67 h PM. The largest differences were found before 27 h PM in agreement with previous studies (Cole et al., 2006; Laurent et al., 2011) and gas composition analyses (Bernaldo de Quirós et al., 2013a). Thus, fatal gas embolism can be distinguished PM from putrefaction gases using gas scoring.

Survivors of the hyperbaric treatment were euthanized after a 1 h observation period. Thus, these animals did not die because of a fatal hyperbaric decompression. They presented a similar gas scoring as the putrefaction model throughout the period of the study. Therefore these animals were able to wash out their nitrogen without causing excessive bubbling during the ascent surface time. We can conclude that the PM quantification of the gas is more relevant from a diagnostic point of view than the mere PM presence or absence of gas.

In many of the papers reporting PM offgassing in humans or animal models, their subjects drowned at depth after hyperbaric conditions or received resuscitation maneuvers (Brown et al., 1978; Cole et al., 2006;

Laurent et al., 2014; Wheen and Williams, 2009). Resuscitation maneuvers are known to introduce gas into circulation (Lawrence and Cooke, 2006). Drowning at depth will impede wash out of nitrogen through respiration during ascent or decompression, thus the gas will necessarily come out of solution and form gas bubbles. This has also been reported for marine mammals and sea turtles accidentally caught in nets (Moore et al., 2009; García-Párraga et al., 2014; Bernaldo de Quirós et al., 2013b). In these cases, a gas scoring might not be helpful since gas bubbles will always form. Further experiments are needed to test if the gas score method would be useful to distinguish between PM offgasing in drowned animals at depth, and *in vivo* gas embolism.

If a marine mammal dies at depth, it will rarely reach the beach until putrefaction gases are formed in sufficient volume to float the animal to the surface, or if hauled up (as in bycatch). In stranded marine mammals other cofounding factors such as catheterizations or resuscitation maneuvers do not take place. Hence, the gas scoring method might be useful to distinguish between putrefaction gases, as the main artifact, and gas embolism in stranded marine mammals. Full pathological studies are needed to distinguish between *in vivo* gas embolism (Fernandez et al., 2005) and a beach cast bycaught animal (Moore et al., 2013). The stranding history might also be extremely helpful in these cases.

The results from the gas score in rabbits could be extrapolated to marine mammals or other species with caution. Temperature and PM time are unknown in most marine mammal strandings. The difference in blood volume, absence or presence of fur, among other factors, might influence the PM time at which macroscopically bubbles could be observed. In order to use the gas score method in marine mammals or other species, a baseline putrefaction (decomposition code) gas scoring needs to be undertaken on that specie. Once the baseline has been built, the pathologist will have to test if his subject has a statistically significant higher gas score than the baseline for that species. Complementary gas composition analyses are highly recommended to support the gas score results.

In this research we have used animal models with the goal of controlling important variables such as the ambient temperature and time of death. The control of these conditions was required in order to test for the efficacy of the method. Given the statistical results obtained, we can conclude that the gas scoring method is a valid diagnostic method, which could be used to distinguish between fatal decompression, iatrogenic air embolism, and putrefaction gases.

In conclusion, we have validated a new low cost, simple technique, which can be used by all stranding networks worldwide, to evaluate the quantity and topography of gas found grossly at necropsies. This method has been proven to be of relevance for distinguishing between different gas embolism processes (*i.e.* iatrogenic air embolism and fatal decompression) from putrefaction gases, especially before 27 h PM. This method would allow for the estimation of the gas quantity in stranded marine mammals which cannot be placed in a CT scanner for logistical reasons. It would be preferable to use the gas score method together with gas analyses to gain maximum data, but the gas score method could also be used as an alternative to gas composition analyses when there is no access to specialized equipment or staff.

Conflict of interest

The authors declare no conflict of interest.

Animal welfare

The study was performed in accordance with all EU applicable laws, regulations, and standards, obtaining the corresponding approval from the different ethical committees.

Acknowledgments

The authors would like to thank all colleagues from the University of Las Palmas de Gran Canaria (Spain) that contributed to this work and to the barophysiology group at the Norwegian University of Science and Technology (Norway) for its scientific contribution. The authors would like also to thank Dr. Michael J. Moore for his continued help and patience editing this paper.

This work was supported by the Spanish Ministry of Science and Innovation with three research projects: AGL 2005-07947, CGL 2009/12663, and CGL 2012-39681 (BOS) as well as the Government of Canary Islands (DG Medio Natural). The Spanish Ministry of Education contributed with personal financial support (the University Professor Formation fellowship). The work was also supported by the Liason Committee between the Central Norway Regional Health Authority (RHA) and the Norwegian University of Science and Technology (NTNU), grant number 46028600.

References

Bajanowski, T., Kohler, H., DuChesne, A., Koops, E., Brinkmann, B., 1998. Proof of air embolism after exhumation. Int. J. Legal Med. 112, 2–7.

Bernaldo de Quirós, Y., 2011. Methodology and Analysis of Gas Embolism: Experimental Models and Stranded Cetaceans (Doctoral thesis). (Las Palmas de Gran Canaria) .

Bernaldo de Quirós, Y., González-Díaz, Ó., Saavedra, P., Arbelo, M., Sierra, E., Sacchini, S., Jepson, P.D., Mazzariol, S., Di Guardo, G., Fernández, A., 2011. Methodology for in situ gas sampling, transport and laboratory analysis of gases from stranded cetaceans. Sci. Report. 1, 193.

Bernaldo de Quirós, Y., González-Diaz, O., Arbelo, M., Sierra, E., Sacchini, S., Fernández, A., 2012a. Decompression vs. decomposition: distribution, amount, and gas composition of bubbles in stranded marine mammals. Front. Physiol. 3.

Bernaldo de Quirós, Y., González-Díaz, Ó., Arbelo, M., Andrada, M., Fernandez, A., 2012b. Protocol for gas sampling and analysis in stranded marine mammals. Protoc. Exch.

Bernaldo de Quirós, Y., González-Díaz, O., Møllerløkken, A., Brubakk, A.O., Hjelde, A., Saavedra, P., Fernández, A., 2013a. Differentiation at autopsy between in vivo gas embolism and putrefaction using gas composition analysis. Int. J. Legal Med. 127, 437–445.

Bernaldo de Quirós, Y., Seewald, J.S., Sylva, S.P., Greer, B., Niemeyer, M., Bogomolni, A.L., Moore, M.J., 2013b. Compositional discrimination of decompression and decomposition gas bubbles in bycaught seals and dolphins. PLoS One 8, e83994.

Bernaldo de Quirós, Y., Seewald, J.S., Sylva, S.P., Greer, B., Niemeyer, M., Bogomolni, A.L., Michael, J.M., 2013c. Compositional discrimination of decompression and decomposition gas bubbles in bycaught seals and dolphins. PLoS One (submitted for publication).

Brown, C.D., Kime, W., Sherrer, E.L., 1978. Postmortem intra-vascular bubbling - decompression artifact. J. Forensic Sci. 23, 511–518.

Cole, A.J., Griffiths, D., Lavender, S., Summers, P., Rich, K., 2006. Relevance of postmortem radiology to the diagnosis of fatal cerebral gas embolism from compressed air diving. J. Clin. Pathol. 59, 489–491.

Dennison, S., Moore, M.J., Fahlman, A., Moore, K., Sharp, S., Harry, C.T., Hoppe, J., Niemeyer, M., Lentell, B., Wells, R.S., 2012. Bubbles in live-stranded dolphins. Proc. R. Soc. B Biol. Sci. 279, 1396–1404.

Eggleton, P., Elsden, J., Feglre, J., Hebb, C.O., 1945. A study of the effects of rapid "decompression" in certain animals. J. Physiol. 104, 129–150.

Fernandez, A., Edwards, J.F., Rodriguez, F., de los Monteros, A.E., Herraez, P., Castro, P., Jaber, J.R., Martin, V., Arbelo, M., 2005. "Gas and fat embolic syndrome" involving a mass stranding of beaked whales (Family Ziphiidae) exposed to anthropogenic sonar signals. Vet. Pathol. 42, 446–457.

García-Párraga, D., Crespo-Picazo, J.L., Bernaldo de Quirós, Y., Cervera, V., Martí-Bonmati, L., Díaz-Delgado, J., Arbelo, M., Moore, M.J., Jepson, P.D., Fernández, A., 2014. Decompression sickness ('the bends') in sea turtles. Dis. Aquat. Org. 111, 191–205.

Geraci, J.R., Lounsbury, V.J., 2005. Marine Mammals Ashore: a Fiel Guide for Strandings. National Aquarium in Baltimore, Baltimore, MD.

Hamilton, R.W., Thalmann, E.D., 2003. Decompression practice. In: Brubakk, A.O., Neuman, T.S. (Eds.), Bennett and Elliott's Physiology and Medicing of Diving, Saunders, pp. 455–500.

Harvey, E.N., 1945. Decompression sickness and bubble fromation in blood and tissues. Bull. N. Y. Acad. Med. 21, 505–536.

Jepson, P.D., Arbelo, M., Deaville, R., Patterson, I.A.P., Castro, P., Baker, J.R., Degollada, E., Ross, H.M., Herraez, P., Pocknell, A.M., Rodriguez, F., Howie, F.E., Espinosa, A., Reid, R.J., Jaber, J.R., Martin, V., Cunningham, A.A., Fernandez, A., 2003. Gas-bubble lesions in stranded cetaceans - was sonar responsible for a spate of whale deaths after an Atlantic military exercise? Nature 425, 575–576.

Jepson, P.D., Deaville, R., Patterson, I.A.P., Pocknell, A.M., Ross, H.M., Baker, J.R., Howie, F.E., Reid, R.J., Colloff, A., Cunningham, A.A., 2005. Acute and chronic gas bubble lesions in cetaceans stranded in the United Kingdom. Vet. Pathol. 42, 291–305.

Knight, B., 1996. Forensic Pathology (London) .

Kuiken, T., García-Hartmann, M., 1991. Dissection techniques and tissues sampling. In: Newsletter (Ed.), 1st European Cetacean Society Workshop on Cetacean Pathology (Leiden, Netherlands).

Laurent, P.-E., Coulange, M., Bartoli, C., Boussuges, A., Rostain, J.-C., Luciano, M., Cohen, F., Rolland, P.-H., Mancini, J., Piercecchi, M.-D., Vidal, V., Gorincour, G., 2011. Appearance of gas collections after scuba diving death: a computed tomography study in a porcine model. Int. J. Legal Med. 127, 177–184.

Laurent, P.-E., Coulange, M., Mancini, J., Bartoli, C., Desfeux, J., Piercecchi-Marti, M.-D., Gorincour, G., 2014. Postmortem CT appearance of gas collections in fatal diving accidents. Am. J. Roentgenol. 203, 468–475.

Lawrence, C., Cooke, C., 2006. Autopsy and the investigation of scuba diving fatalities. Diving and Hyperbaric Medicine - South Pacific Underwater Medicine Society. Vol. 36, pp. 2–8.

Lever, M.J., Miller, K.W., Paton, W.D.M., Smith, E.B., 1966. Experiments on the genesis of bubbles as a result of rapid decompression. J. Physiol. 184, 964–969.

Moore, M.J., Early, G.A., 2004. Cumulative sperm whale bone damage and the bends. Science 306, 2215-2215.

Moore, M.J., Bogomolni, A.L., Dennison, S.E., Early, G., Garner, M.M., Hayward, B.A., Lentell, B.J., Rotstein, D.S., 2009. Gas bubbles in seals, dolphins, and porpoises entangled and drowned at depth in gillnets. Vet. Pathol. 46, 536–547.

Moore, M.J., van der Hoop, J., Barco, S.G., Costidis, A.M., Gulland, F.M., Jepson, P.D., Moore, K.T., Raverty, S., McLellan, W.A., 2013. Criteria and case definitions for serious injury and death of pinnipeds and cetaceans caused by anthropogenic trauma. Dis. Aquat. Org. 103, 229–264.

Muth, C.M., Shank, E.S., 2000. Primary care: gas embolism. N. Engl. J. Med. 342, 476–482.

Richter, M., 1905. Gerichtsärztliche Diagnostik und Technik. S. Hirzel, Leipzig.

Shim, S.S., Patterson, F.P., Kendall, M.J., 1967. Hyperbaric chamber and decompression sickness: an experimental study. Can. Med. Assoc. J. 97, 1263–1272.

Varlet, V., Bruguier, C., Grabherr, S., Augsburger, M., Mangin, P., Uldin, T., 2014. Gas analysis of exhumed cadavers buried for 30 years: a case report about long time alteration. Int. J. Legal Med. 128, 719–724.

Varlet, V., Smith, F., Giuliani, N., Egger, C., Rinaldi, A., Dominguez, A., Chevallier, C., Bruguier, C., Augsburger, M., Mangin, P., Grabherr, S., 2015. When gas analysis assists with postmortem imaging to diagnose causes of death. Forensic Sci. Int. 251, 1–10.

Wheen, L.C., Williams, M.P., 2009. Post-mortems in recreational scuba diver deaths: the utility of radiology. J. Forensic Legal Med. 16, 273–276.

Yokota, H., Yamamoto, S., Horikoshi, T., Shimofusa, R., Ito, H., 2009. What is the origin of intravascular gas on postmortem computed tomography? Legal Med. 11 (Suppl. 1), S252–S255 (Tokyo).